

Fig. S1. SNX19 loss does not affect autophagy (A) Snz:GFP-expressing flies in the presence and absence of snz RNAi. Images are representative of three independent experiments. (B) Representative images of LyTr-stained fed and starved fat bodies overexpressing snz:GFP. (C). Mean LyTr objects normalized to the tissue area. Bars represent the mean, individual points represent single fat body values, and the error bars are the SEM ($n=4$ independent experiments). (D) qRT-PCR validation of SNX19 siRNA efficiencies. Reactions were normalized to control, which were set at 1. (E) Anti-LC3 western blots of SNX19 siRNA-transfected HeLa cells grown in full DMEM treated with or without bafilomycin A1. Tubulin was used as a loading control. $n=3$ independent experiments (F) Immunofluorescence analysis of endogenous LC3 (green) in scramble or SNX19 siRNA-transfected HeLa cells grown in full DMEM with or without bafilomycin A1 (BafA1) treatment. Nuclei were counterstained with 4',6-diamidino-2-phenylindole (DAPI). Images are representative of three independent experiments. (G) Quantification of LC3 puncta per cell. Bars represent the mean, individual points or triangles represent single-cell values, and the error bars are the SEM ($n=3$ independent experiments).

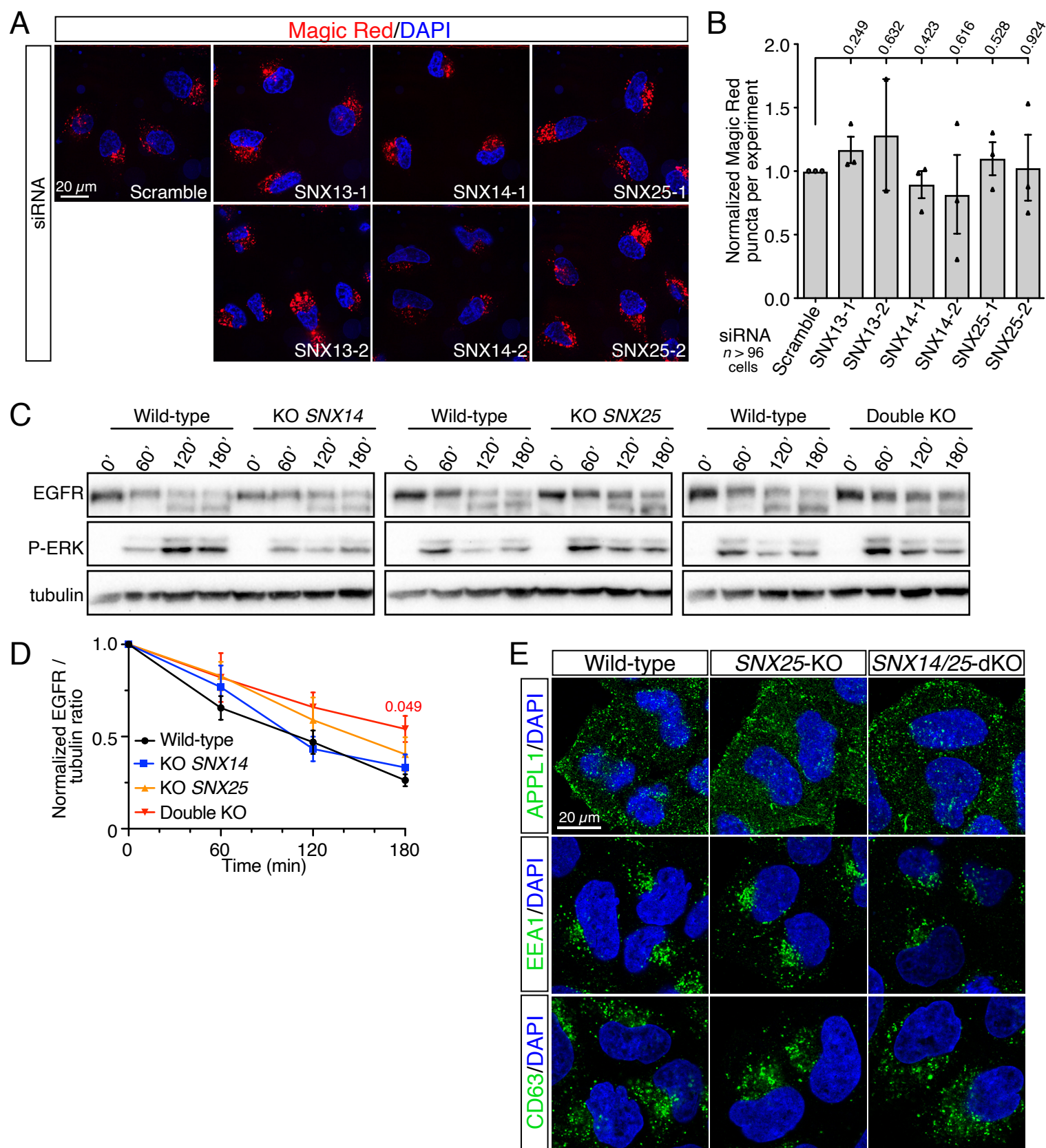


Fig. S2. *SNX14* and *SNX25* loss modestly impairs lysosomal functions (A) Representative images of Magic Red staining to detect cathepsin B activity in HeLa cells transfected with siRNAs against *SNX13*, *SNX14*, and *SNX25*. (B) Quantification of the normalized number of Magic Red puncta per experiment. Bars represent the mean, individual points or triangles represent single experimental values, and the error bars are the SEM ($n=3$ independent experiments). (C) Effects of *SNX14*, *SNX25*, and *SNX14/SNX25* KO on EGFR activation and degradation after stimulation with 100 nM EGF. (D) Normalized integrated density ratios of EGFR to tubulin in the various HeLa KO populations. Error bars are the SEM ($n=3$ independent experiments). (E) Representative immunofluorescent images of *SNX25* KO and *SNX14/SNX25* double KO cells stained for APPL1, EEA1, and CD63 and counterstained with DAPI.

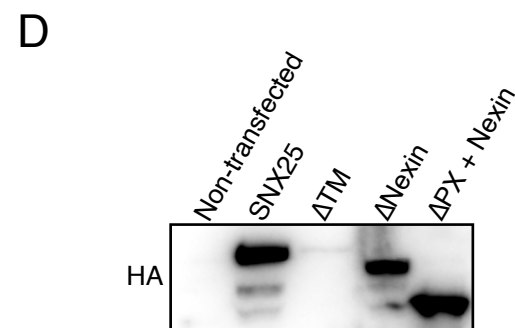
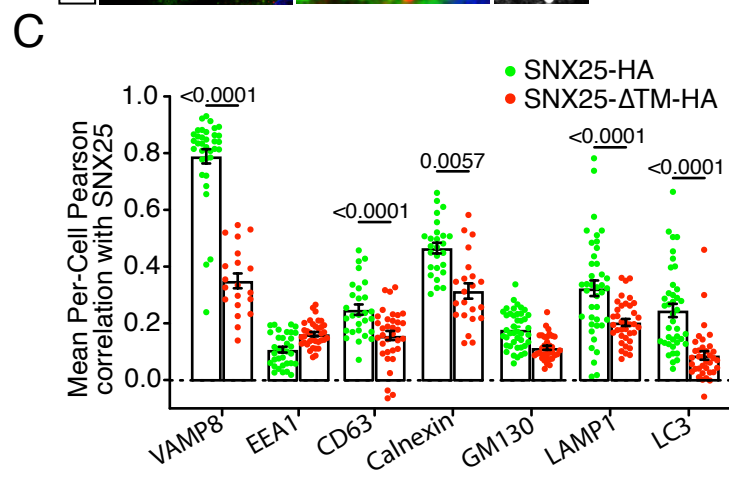
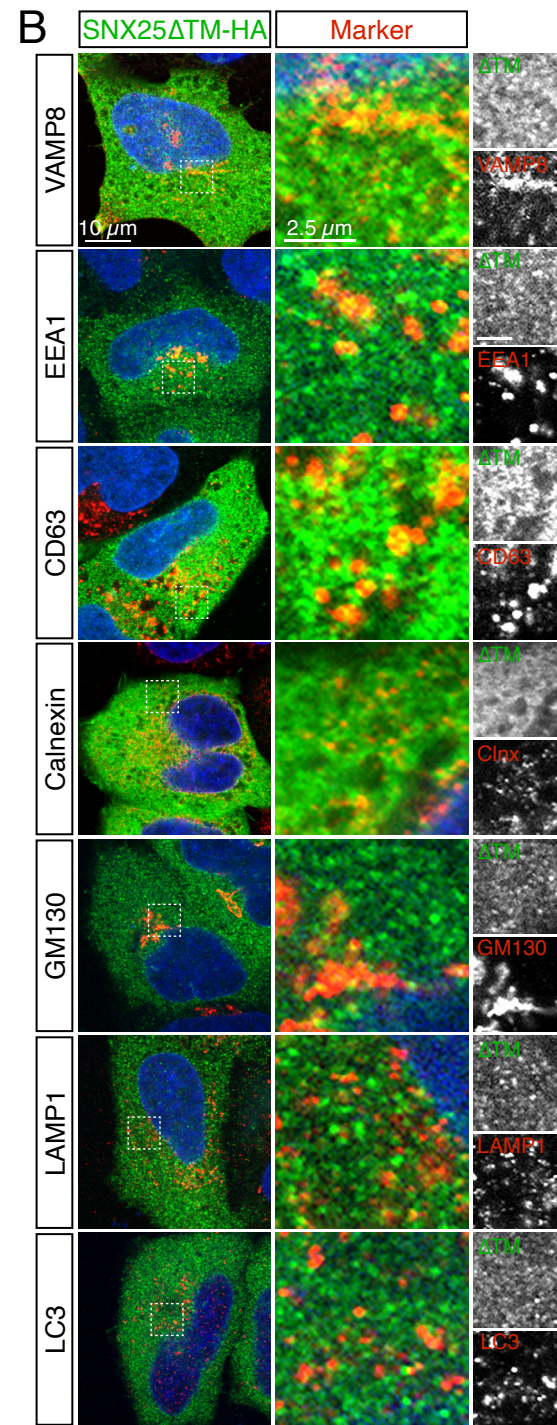
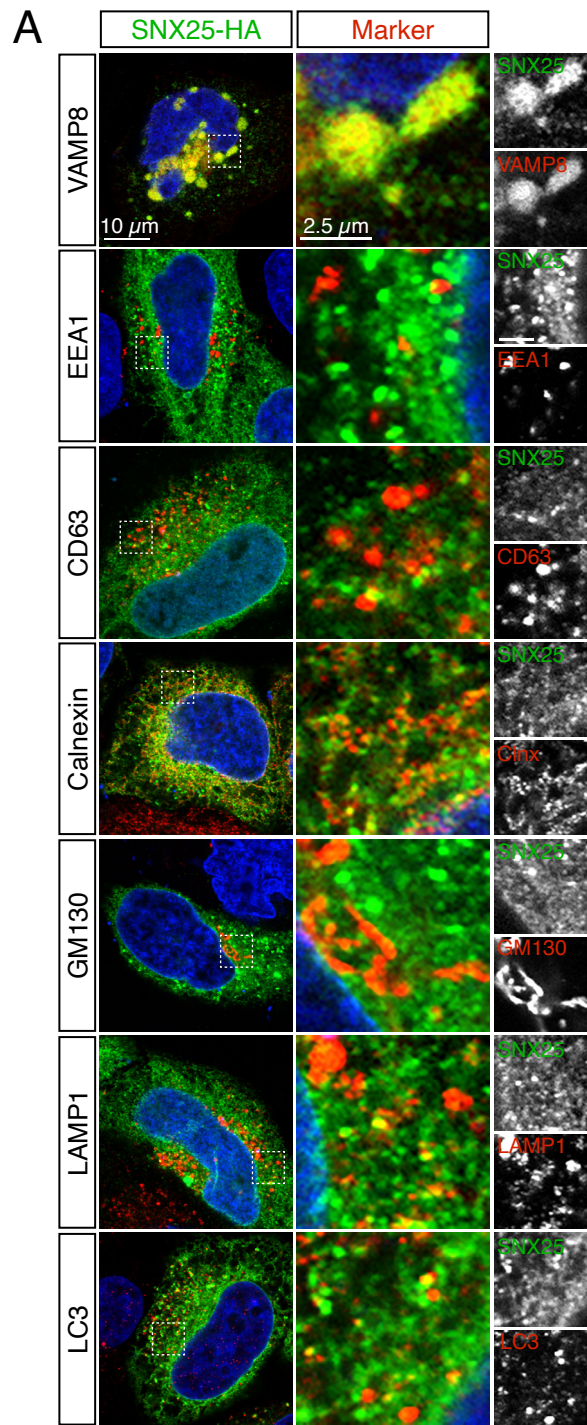


Fig. S3. SNX25 strongly colocalizes with VAMP8 and to some degree with other cellular compartments (A and B) Representative immunofluorescent images of cells transfected with (A) full-length SNX25-HA and (B) SNX25- Δ TM-HA, which lacks the TM domains. Cells were either co-transfected with VAMP8-GFP or immunostained for EEA1, CD63, calnexin, GM130, LAMP1, or LC3. (C) Per-cell Pearson's correlations between SNX25-HA/SNX25- Δ TM-HA and the various markers. Bars represent the mean, individual points represent single-cell values, and the error bars are the SEM ($n=3$ independent experiments). (D) Anti-HA western blot of SNX25 constructs used in the KO/rescue experiments.

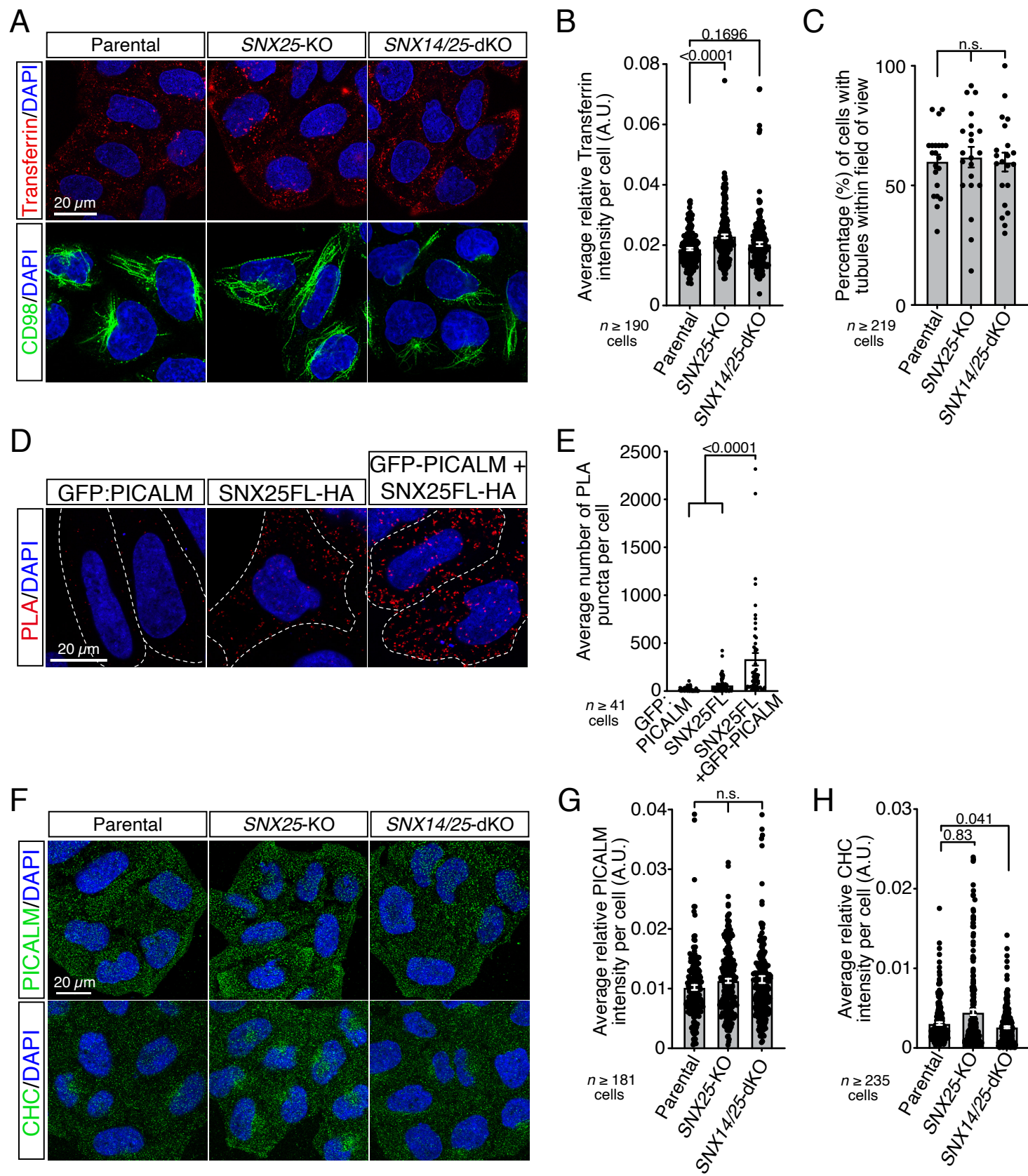


Fig. S4. SNX25 is dispensable for clathrin-dependent and -independent endocytosis and PICALM recruitment (A) Transferrin and CD98 uptake in WT, *SNX25* KO, and *SNX14/25* double KO cells. Cells were acid-washed for both uptakes and before fixation to assess only internalized transferrin and CD98. (B and C) Average per-cell transferrin intensity (B) and percentage of cells with tubules (C). Bars represent the mean, individual points represent single-cell values, and the error bars are the SEM ($n=3$ independent experiments). (D) PLA immunofluorescence shows the respective proximities between GFP-PICALM and SNX25FL-HA. GFP-PICALM and SNX25FL-HA were also transfected individually and probed with both antibodies as PLA controls (first two panels). PLA puncta are shown in red and nuclei in blue. Dotted lines define individual cells. (E) Quantification of the PLA shown in D. Bars represent the average number of PLA puncta per cell, individual points represent single cells, and the error bars are the SEM ($n=3$ independent experiments). (F) Immunofluorescence analysis of PICALM and clathrin heavy chain (CHC) in parental and KO cells. Confocal images were acquired on the ventral side of cells to image PM-localized PICALM and CHC. (G and H) Average per-cell PICALM (G) and CHC (H) intensities. Bars represent the mean, individual points represent single-cell values, and the error bars are the SEM ($n=3$ independent experiments). A.U., arbitrary units, n.s., not significant.

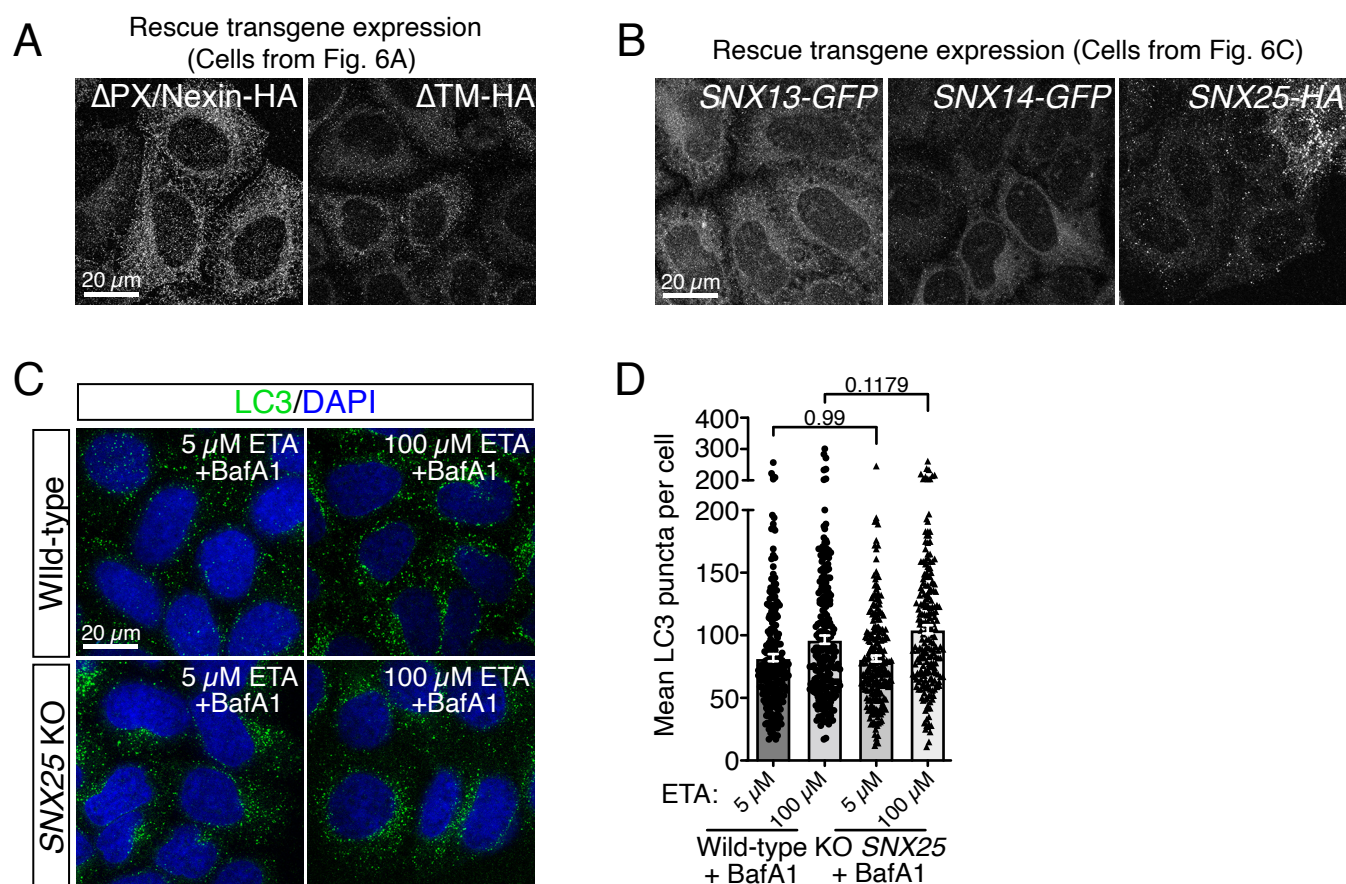


Fig. S5. Ethanolamine addition does not affect autophagosome formation (A) HA immunofluorescence of SNX25 KO cells expressing the Δ PX/ Δ Nexin-HA or Δ TM-HA mutants. (B) GFP fluorescence of SNX13-GFP or SNX14-GFP and anti-HA immunofluorescence of SNX25-HA in SNX25 KO cells. (C) Immunofluorescence analysis of endogenous LC3 (green) in parental of SNX25 KO HeLa cells grown in full DMEM with or without bafilomycin A1 (BafA1) treatment supplement with two concentrations of ETA for 24 hours prior cell fixation. Nuclei were counterstained with 4',6-diamidino-2-phenylindole (DAPI). Images are representative of three independent experiments. Parental HeLa cells were stained for LC3 in the same experimental sets to validate the BafA1 treatment (mean number of LC3 puncta per cell was 18.75 ± 0.83 (SEM)) (D) Quantification of LC3 puncta per cell. Bars represent the mean, individual points or triangles represent single-cell values, and the error bars are the SEM ($n=3$ independent experiments).

Table S1. List of primers used for ddPCR reactions

[Click here to download Table S1](#)